Immune Cell PD-L1 Colocalizes with Macrophages and Is Associated with Outcome in PD-1 Pathway Blockade Therapy

Yuting Liu[1], Jon Zugazagoitia[1], Fahad Shabbir Ahmed[1], Brian S. Henick[2], Scott N. Gettinger[3], Roy S. Herbst[3], Kurt A. Schalper[1,3], and David L. Rimm[1,3]

ABSTRACT

Purpose: Programmed death ligand 1 (PD-L1) is expressed in tumor cells and immune cells, and both have been associated with response to anti-PD-1 axis immunotherapy. Here, we examine the expression of PD-L1 to determine which cell type carries the predictive value of the test.

Experimental Design: We measured the expression of PD-L1 in multiple immune cells with two platforms and confocal microscopy on three retrospective Yale NSCLC cohorts (425 nonimmunotherapy-treated cases and 62 pembrolizumab/nivolumab/atezolizumab-treated cases). The PD-L1 level was selectively measured in different immune cell subsets using two multiplexed quantitative immunofluorescence panels, including CD56 for natural killer cells, CD68 for macrophages, and CD8 for cytotoxic T cells.

Results: PD-L1 was significantly higher in macrophages in both tumor and stromal compartment compared with other immune cells. Elevated PD-L1 in macrophages was correlated with high PD-L1 level in tumor as well as CD8 and CD68 level ($P < 0.0001$). High PD-L1 expression in macrophages was correlated with better overall survival (OS; $P = 0.036$ by cell count/$P = 0.019$ by molecular colocalization), while high PD-L1 expression in tumor cells was not.

Conclusions: In nearly 500 non–small cell lung cancer (NSCLC) cases, the predominant immune cell type that expresses PD-L1 is $CD68^+$ macrophages. The level of PD-L1 in macrophages is significantly associated with the level of PD-L1 in tumor cells and infiltration by $CD8^+$ T cells, suggesting a connection between high PD-L1 and "hot" tumors. In anti-PD-1 axis therapy–treated patients, high levels of PD-L1 expression in macrophages are associated with longer OS and may be responsible for the predictive effect of the marker.

Introduction

Immune checkpoints are regulators of the immune system and they are crucial for maintaining the immune homeostasis by controlling the amplitude of immune responses (1). In cancer, immune checkpoints are often expressed by tumor cells to suppress the antitumor immune responses against them as an adaptive escape mechanism (2, 3). Among the discovered immune checkpoints, the interaction between programmed death 1 receptor (PD-1) on tumor infiltrating lymphocytes (TIL) and its ligand programmed death ligand 1 (PD-L1) on tumor cells has been identified as a critical immunosuppressive mechanism in cancer (4–6).

Several clinical studies have shown that antibodies targeting PD-1/PD-L1 pathway achieved durable clinical responses with unprecedented survival rate (7, 8). However, only a fraction of patients benefit from this therapy and some of the therapies are approved with a companion diagnostic test to identify patients who are more likely to respond. The only currently FDA-approved companion diagnostic is the PD-L1 IHC test (9). A number of IHC tests are approved with varied antibody clones, staining platforms, protocols and scoring system, and the localization of PD-L1 detection. The first approved test (22c3) scored only PD-L1 expression on tumor cells while other assays, for example, the SP142 assay prescribed scoring of both tumor cells and immune cells. More recently, in tumors other than non–small cell lung cancer (NSCLC), the 22c3 test has evolved to a combined proportion score that includes both tumor cells and immune cells. The evolution toward inclusion of PD-L1 detection on immune cells in diagnostics reveals its importance to anti-PD-1 therapeutic efficacy as compared with PD-L1 expression by tumor cells. This evolution of diagnostic scoring coincides with recent work in mouse models that has shown the efficacy of anti-PD-1 axis blockade relies on the host expression of PD-L1 in the tumor microenvironment and draining lymph nodes rather than in tumor cells (10–12).

In this study, we follow the mouse mechanistic studies to attempt to determine the cell type in which the PD-L1 expression is associated with the drug mechanism of action. We hypothesize that the immune cells scored in the tests are predominantly macrophages and that the expression of PD-L1 in these cells is the critical target for immune therapy and therefore the best target for future assessment.

Materials and Methods

Tissue microarray and patient cohorts

Discovery cohort

We used two retrospective collections of NSCLC from Yale University, cohort A (YTMA79; $n = 209$) and cohort B (YTMA250; $n = 291$), that consist of 500 patients from 1988 to 2003 (YTMA79) and 2004 to 2011 (YTMA250) as described previously (13, 14). Detailed clinicopathologic characterization is summarized in Supplementary Table S1. The cases that were finally included in the study were fewer

[1]Department of Pathology, Yale University School of Medicine, New Haven, Connecticut. [2]Department of Medicine (Oncology), Columbia University Medical Center, New York, New York. [3]Department of Medicine (Oncology), Yale University School of Medicine, New Haven, Connecticut.

Note: Supplementary data for this article are available at Clinical Cancer Research Online (http://clincancerres.aacrjournals.org/).

Corresponding Author: David L. Rimm, Yale School of Medicine, PO Box 208023, 310 Cedar Street, New Haven, CT 06520-8023. Phone: 203-737-4204; E-mail: david.rimm@yale.edu

Clin Cancer Res 2020;26:970–7

doi: 10.1158/1078-0432.CCR-19-1040

Translational Relevance

Many studies have shown that "immune cells," without specific characterization, are a critical component of the companion diagnostic tests used for programmed death 1 receptor (PD-1) axis immunotherapy. The exact type of immune cells that express programmed death ligand 1 (PD-L1) is unclear. By quantitatively measuring PD-L1 in $CD68^+$ macrophages, $CD56^+$ natural killer cells, and $CD8^+$ cytotoxic T cells we show that the vast majority of PD-L1 expression colocalizes with CD68, inferring that the key immune cell is a macrophage. It is more challenging to prove that the macrophage carries the predictive power of the test. However, in a small pilot scale, retrospective cohort, we show significant association with overall survival attributable to PD-L1 in the macrophage compartment, and not in the tumor cell compartment. This work raises the possibility that the companion diagnostic test for PD-1 axis therapies may be improved by assessing PD-L1 expression only when it is colocalized with CD68.

(176/209 in YTMA79; 249/291 in YTMA250) due to the loss of tissue, missing data, or poor quality of the staining as seen in other TMA studies. All tissue samples were collected with the approval from the Yale Human Investigation committee protocol #9505008219. The Yale Human Investigation Committee approved the patient consent forms or in some cases a waiver of consent all in accordance with the ethical guidelines of the U.S. Common Rule.

All tissue specimens from the two cohorts were obtained from formalin-fixed, paraffin embedded (FFPE) tissue and were prepared as a tissue microarray (TMA) with a previously described standard procedure (15, 16). FFPE cell line pellets were used as controls. For each TMAs, we used two different blocks containing different tumor areas of the same tumors. For analysis, spots from the same patients were averaged.

Immunotherapy treated cohort

We used tumor samples from patients with NSCLC, cohort C (YTMA404; $n = 81$) treated with anti-PD-1 axis therapy at Yale-New Haven Hospital between 2011 and 2018. As summarized in **Table 1**, 62 of 81 samples were collected before immunotherapy and treated with single-agent therapy (pembrolizumab, nivolumab, or atezolizumab). All tissue specimens were obtained from FFPE biopsy or resection tissue and prepared as TMA. Response status was determined using RECIST v1.1 criteria.

Control cohort

We used a control cohort YTMA337, which is a specially selected PD-L1–specific index array NSCLC tumors ($n = 30$) and cell line pellets with variable levels of PD-L1 expression in 2-fold redundancy. For standardization, we stained YTMA337 alongside with each experiment as quality control to show that the YTMA337 staining pattern is quantitatively consistent between experiments.

Antibody validation

CD68 antibody (1:200; Mouse monoclonal, IgG3, clone PG-M1, DAKO) and CD8 antibody (1:250; Mouse monoclonal, IgG1, clone C8/144B, DAKO) were validated in our laboratory and published previously (17, 18). CD56 antibody (1:200; Mouse monoclonal, IgG1, clone 123C3, DAKO) was cross-validated with antibody clone 56C04

Table 1. Immunotherapy Treated Cohort Characteristics.

Characteristics	*N* (%)
Total	81
Gender	
Male	43 (53.1)
Female	38 (46.9)
Age	
<70 years old	42 (51.9)
≥70 years old	39 (48.1)
Smoking history	
Never smoker	14 (17.3)
Current smoker	18 (22.2)
Former smoker	48 (59.3)
Missing	1
Histology	
Adenocarcinoma	61 (75.3)
Squamous cell carcinoma	15 (18.5)
Large cell carcinoma	4 (4.9)
Adenosquamous carcinoma	1 (1.2)
Stage	
III	2 (2.5)
IV (M1a)	21 (25.9)
IV (M1b)	11 (13.6)
IV (M1c)	47 (58)
Actionable drivers	
Yes	37 (45.7)
EGFR mutation	11 (13.6)
KRAS mutation	21 (25.9)
MET amplification	1 (1.2)
RET fusion	1 (1.2)
HER2 mutation	1 (1.2)
MEK1 mutation	1 (1.2)
PIK3CA mutation	1 (1.2)
No	44 (54.3)
Genotype-tailored therapies	
Yes	13 (16)
No	68 (84)
Site	
Lung primary	41 (50.6)
Locoregional lymph node	14 (17.3)
Metastatic (M1) lymph node	4 (4.9)
Brain metastasis	10 (12.3)
Adrenal metastasis	2 (2.5)
Pleural metastasis	1 (1.2)
Renal metastasis	1 (1.2)
Skeletal soft tissue metastasis	4 (4.9)
Skin metastasis	1 (1.2)
Pericardium	1 (1.2)
Thoracic spine	1 (1.2)
Missing	1
N lines of therapy	
0	16 (19.8)
1	42 (51.9)
2	19 (23.5)
3	2 (2.5)
4	1 (1.2)
Missing	1
Radiotherapy prior to immunotherapy	
Yes	28 (34.6)
No	53 (65.4)
Moment of collection	
Preimmunotherapy	73 (90.1)
Postimmunotherapy	8 (9.9)

(Continued on the following page)

Table 1. Immunotherapy Treated Cohort Characteristics. (Cont'd)

Characteristics	*N* (%)
Immunotherapy regimens	
Nivolumab	57 (70.4)
Pembrolizumab	5 (6.2)
Atezolizumab	5 (6.2)
Others	14 (17.2)

(1:100, Mouse monoclonal, Thermo Fisher Scientific). Both CD56 antibodies were evaluated on the control cohort with immunofluorescence (IF). Comparison between two clones shows a high regression coefficient ($R^2 > 0.7$). This combined with vendor specificity validation assured to CD56 antibody validation. CD8 assays were validated in previous studies.

Quantitative immunofluorescence

TMA slides were baked at 60°C for 1 hour and then soaked in xylene twice for 20 minutes each. Rehydration was performed with two 1-minute washes in 100% ethanol followed by 1-minute wash in 70% ethanol and 5-minute rinse under streaming tap water. Antigen retrieval was then performed with pH 8 EDTA buffer for 20 minutes at 97°C in the Lab Vision PT Module (Thermo Fisher Scientific). Thirty-minute incubation in 2.5% hydrogen peroxide in methanol was performed to block endogenous peroxidases and subsequently unspecific antigens were blocked using a 0.3% BSA in Tris Base Saline Tween (TBST) for 30 minutes. For the PD-L1/CD68/CD8 multiplex panel, a cocktail of primary antibodies including PD-L1 (1:800; Rabbit monoclonal, clone SP142, Spring), CD68, and CD8 were incubated in 0.3%BSA in TBST overnight at 4○C. Horseradish peroxidases (HRP)-conjugated secondary antibodies specific to each primary antibody isotype were used sequentially (anti-mouse IgG3, 1:1,000, Abcam; anti-rabbit EnVision, DAKO; anti-mouse IgG1, 1:100, eBioscience). Note that the primary antibody used for PD-L1 here is the SP142 antibody, not the SP142 assay. In other works, the antibody has been shown to be equivalent to other cytoplasmic domain PD-L1 antibodies (19), even though the assay has proven to be of lower sensitivity (20, 21). Tyramide-bound fluorophores were added after each secondary antibody to bind to the HRPs. Specifically, biotinylated tyramide (1:50, PerkinElmer) and Alexa750-streptavidin (1:100, Life Technologies) were used for CD68, Cyanine 5 (Cy5) tyramide (1:50, PerkinElmer) was used for PD-L1, and Cy3 tyramide plus (1:100, PerkinElmer) was used for CD8. Epithelial tumor cells were detected with 1-hour incubation of anti-rabbit pan-cytokeratin(CK) (1:100, DAKO) and following 1-hour incubation of goat-anti-rabbit Alexa488 (1:100; eBioscience) at room temperature. Finally, nucleus was stained with 4,6-diamidino-2-phenylin-dole (DAPI; 1:1,000, Life Technologies) for 10 minutes at room temperature and mounted with Prolong Gold Mounting Reagent (Life Technologies). For the PD-L1/CD68/CD56 multiplex panel, a cocktail of primary antibodies including PD-L1, CD68, and CD56 were used and the rest of the protocol is the same as previously described.

Quantitative immunofluorescence (QIF) was quantified using two platforms: image collection was done on either the PM2000 (HistoRx) or Vectra Polaris (Perkin Elmer) automated fluorescence microscopy platforms. The resultant images were analyzed and quantified using either the AQUAnalysis Software (Navigate Biopharma) or the InForm Software (Perkin Elmer) on all tumor spots as described previously (13). Briefly, fluorescent images of DAPI, FITC (CK), Cy5 (PD-L1) Cy3 (CD56/CD8), and Cy7 (CD68) for each core were collected on either platform except for the Vectra Polaris, multispectral images were captured in five channels on all tumor spots. With the trainable feature-recognition inForm software, specific cells and tissue types were identified. The cell count for phenotype of interest (PD-L1 and CD68/CD8/CD56 double-positive phenotype) was calculated in both tumor and stromal tissue for final analysis. All acquired tumor spots were evaluated visually and spots with less than 2% of tumor or staining artifacts were excluded from the final analysis. An AQUA score of 500 AU was used to define PD-L1 positivity to reproduce a 1% TPS threshold and was determined by visualization of IF staining of PD-L1.

DNA-tagged QIF

We stained one slide from the same NSCLC TMA cohort C block with the Ultimapper Kit (Ultivue Inc). The slide was deparaffinized in an oven at 60°C (oven company) for 20 minutes followed by immediate immersion in xylene (twice) for 20 minutes each. The slide was rehydrated using graded alcohols (100%, 100%, 70% ethanol) followed by tap water. Antigen retrieval was done using EDTA (company) at pH 9 in a PT Module pressure boiler with preheating the solution to 85°C then 20 minutes at 97°C followed by cooling at 75°C, and then the module tank was kept under running tap water for 10 minutes. The slide was then washed in PBS thrice by submersion. Blocking was done using the blocking solution in the Ultimapper kit at room temperature (20°C–25°C) for 15 minutes in a humid chamber. The antibody solution was made (mixing of single-strand DNA-tagged antibodies and antibody diluent) and intubated for 60 minutes at room temperature in a humid chamber. Amplification of the DNA strand was done with preamplification solution for 25 minutes at room temperature in humid chamber followed by Amplification solution (Amplification enzyme and Amplification buffer) at 30°C in a sealed humid chamber (Slide Moat, Boekel Scientific). This was followed by nuclear staining (Hoescht) and amplification of fluorescent-tagged DNA probes for 25 minutes at room temperature. The slides where then cover slipped and scanned using the PM2000 machines and AQUA Scores were generated for each marker and studied for the impact on overall survival (OS).

Confocal microscopy

For high resolution images, the TMA slides were examined using a Leica SP5 Confocal Microscope at 100× magnification in the fluorescent mode. Image acquisition and analysis were performed on the LAS AS Software (Leica). The excitation and emission wavelengths used to detect were at 405 nm, 561 nm, 633 nm, and a multi-line Argon.

Statistical analysis

Reproducibility of the assays is measured with the control cohort with Pearson correlation coefficient (*R*). An AQUA score of 500 AU was used to stratify PD-L1 SP142 staining scores into positive or negative groups of patients for analysis. This threshold was determined with visual inspection of all NSCLC tumor cohorts and the control array. AQUA scores and inForm cell counts between responders (partial response/complete response) and nonresponders (stable disease/progressive disease) were compared with Fisher exact test two-sided. Survival analysis was carried out using Kaplan–Meier curves and significance was determined with the log-rank test. Joinpoint 4.6.0.0 was used to identify the marker score, which is an apparent change in trend that is statistically significant without referring to the outcome data (22). The univariate analyses were performed with GraphPad Prism 7, and multivariate analyses were performed using JMP11. All *P* values were descriptive and based on two-sided tests and were not adjusted for multiple comparisons.

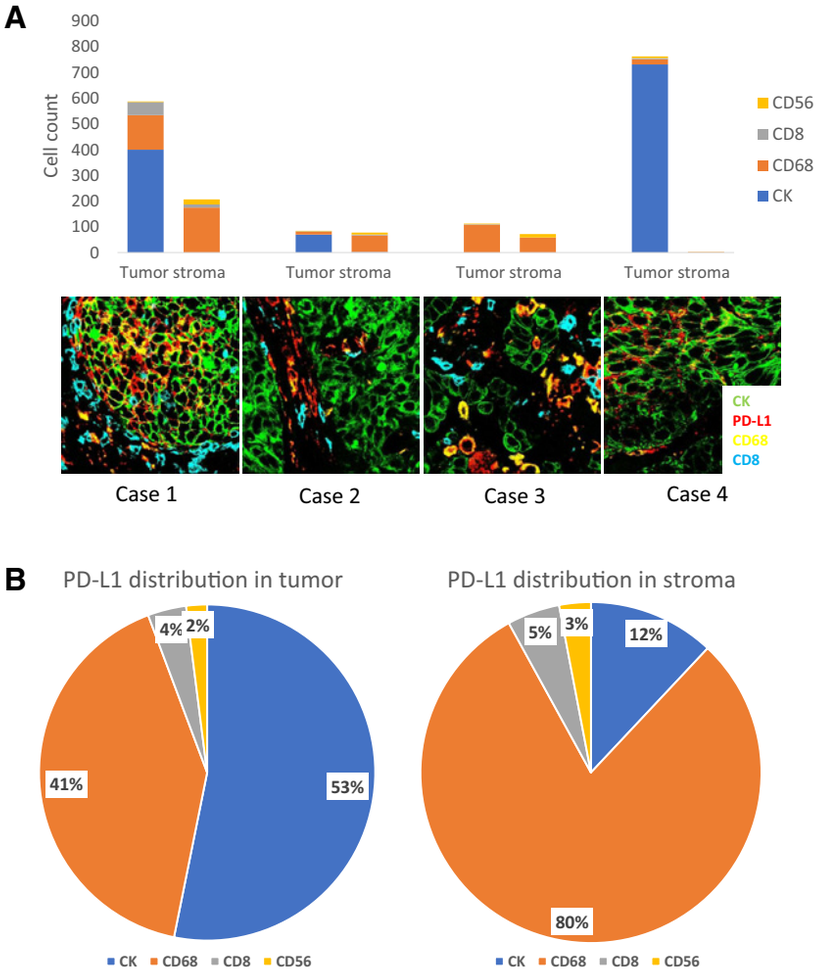

Figure 1.

A, Quantification of PD-L1 localization in tumor and stroma. Four representative cases to demonstrate typical PD-L1 localization patterns with cell counts and confocal images of regions of the counted case. **B,** Summary pie charts of PD-L1 localization calculated by double positive phenotype cell counts (PD-L1/CK, PD-L1/CD68, PD-L1/CD8, and PD-L1/CD56) on the average of 457 NSCLC cases were presented as percentages in both tumor and stromal compartment.

Results

Among the 425 NSCLC cases in discovery cohorts A and B, $CD68^+$, CK^- cells, defined as macrophages were present in 391 of 425 (92%) cases, while $CD8^+$, CK^- T cells and $CD56^+$, CK^- natural killer (NK) cells were present in 388 of 425 (91.3%) and 90 of 209 (43.1%), respectively. A visually estimated threshold of 500 arbitrary units of fluorescence (au) of AQUA score was used to determine the patients into PD-L1–positive (126/425, 29.6%) or -negative group (299/425, 70.4%). Then inForm was used to assess PD-L1 expression on both tumor tissue compartment and stromal tissue compartment where tumor was defined by a machine learning algorithm that defines CK-positive regions as tumor tissue compartment. A similar training approach was used for the stromal compartment definition using DAPI and absence of CK. Finally, a third compartment was defined/trained, where there is no tissue. PD-L1 cellular localization was then determined within the PD-L1–positive group (determined by AQUA, $n = 126$) by the cell count of the following phenotype: PD-L1/CK double positive, PD-L1/CD68 double positive, PD-L1/CD56 double positive, and PD-L1/CD8 double positive in both tumor and stromal compartments. **Figure 1A** illustrates a series of case examples. Case 1, where tumor PD-L1 was predominantly localized with CK, also showing some expression in tumor-infiltrating macrophages. Case 2 shows PD-L1 localization with CK in the tumor compartment and with CD68 in stromal compartment. Case 3 shows PD-L1 was only localized with CD68 in both tumor and stromal. Finally, case 4 shows PD-L1 only expressed by CK in the tumor compartment. Then these data were averaged across 126 cases of PD-L1–positive NSCLC and shown in summary pie charts in **Fig. 1B**. PD-L1 localization was significantly higher in $CD68^+$ macrophages compared with $CD56^+$ NK cells and $CD8^+$ T cells: in the tumor compartment, PD-L1 was predominantly colocalized with CK (53%) while 41% of PD-L1 was found to be colocalized with CD68, 4% with CD8, and 2% with CD56; in the stromal compartment, the majority of PD-L1–positive cells were CD68 positive (80%), while only 5% from CD8, and 3% from CD56.

To better illustrate the compartmentalization of PD-L1 expression, **Fig. 2** shows high magnification confocal images of four examples, both combined and separated by the channel along with the same region stained with hematoxylin and eosin after capturing the fluorescent images and the chromogenic IHC image from a serial section of the same tissue region. Note that it is hard to visualize the colocalization in either the CD8 or CD56 compartments because they represent a relatively small percentage of the total PD-L1. Because the PD-L1 expression in this study was mainly found in CK and $CD68^+$ cells, and PD-L1 in CD56 and CD8 was relatively low, the remainder of this work focuses on the expression of PD-L1 by tumor cell and $CD68^+$ macrophage only. Correlation between PD-L1 level in $CD68^+$ macrophages and PD-L1 level in tumor, CD8 and CD68 levels was identified,

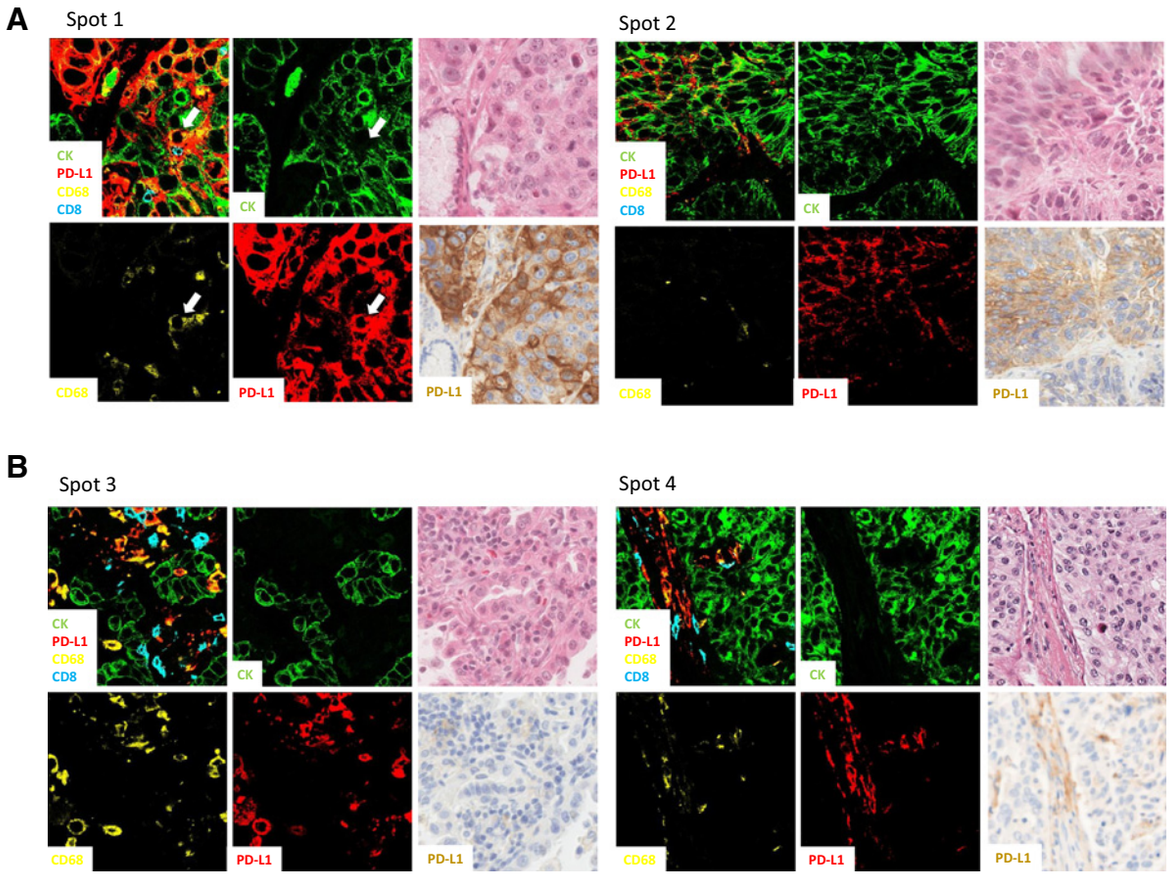

Figure 2.

Colocalization of phenotypic markers and PD-L1. Example confocal images of PD-L1 colocalization with tumor cells (**A**) and with macrophages (**B**). **A,** White arrow is a tumor-infiltrating macrophage with CD68 and PD-L1 double staining, but without cytokeratin staining.

indicating a connection between high PD-L1 level in macrophages and "hot" tumors (Supplementary Fig. S1).

Next, we assessed the association with outcome for PD-L1 expression in each compartment. The potential correlation between the prognostic value of PD-L1 level in macrophages and patients' outcome was evaluated in a merged analysis of Yale cohorts A and B. No significant association between PD-L1 level in macrophages and major clinicopathologic variables was found. PD-L1 expression in $CD68^+$ macrophages was defined as cases where PD-L1 expression level was above a visual threshold of 3,000 au of AQUA score (156/425, 36.7%). The remainder of the cases were PD-L1 negative in macrophage group (269/425, 63.3%). High PD-L1 expression in macrophages was significantly associated with high PD-L1 level in tumor, as well as CD8 level and CD68 level ($P < 0.0001$; **Fig. 3A**). With the median cutoff, or any discovered cut-off point, we found PD-L1 level in CD68 was not associated with patient's survival in patients treated with standard-of-care therapy received by the patients in these retrospective cohorts gathered prior to the availability of immune therapy (**Fig. 3B**, Supplementary Figs. S2 and S3).

The potential predictive value of PD-L1 in macrophages was evaluated in Yale cohort C, the immunotherapy-treated cohort. The joinpoint method is independent of outcome (22), so it was used to define a cohort stratification threshold. With the normalized cell count of total PD-L1/CK double–positive phenotype and PD-L1/CD68 double–positive phenotype, a joinpoint analysis for natural population breaks identified a significant breakpoint at the 25th percentile of the PD-L1/CK cell count ($n = 15$; total $n = 59$; $P = 0.00222$) and the 21st percentile of the PD-L1/CD68 cell count within total cell count ($n = 12$; total $n = 61$; $P = 0.00222$; Supplementary Fig. S5). With these joinpoints, no predictive value was found for high cell count for the PD-L1/CK phenotype (**Fig. 4A**), while high cell count of PD-L1/CD68 phenotype was associated with better OS in patients treated with single therapy (pembrolizumab/nivolumab/atezolizumab; $P = 0.036$; **Fig. 4B**). Multivariate analysis indicated that the predictive value of high cell count of PD-L1/CD68 phenotype toward OS was independent of age, sex, stage smoking history, and CD8 level (Supplementary Table S3). No significance was found between the PD-L1 level in $CD68^+$ macrophages and response to immunotherapy or progression-free survival in this small cohort.

To confirm this observation, a second independent assay method was used using DNA-based QIF on the same Yale cohort C. This method uses different antibodies and no secondary antibodies, but rather a direct labeling of primary antibodies with oligonucleotide codes. These oligonucleotides provide specificity and can be differentially amplified and assessed by multiplex QIF using either the AQUA method, inForm method, or other QIF methods. The antibodies in the

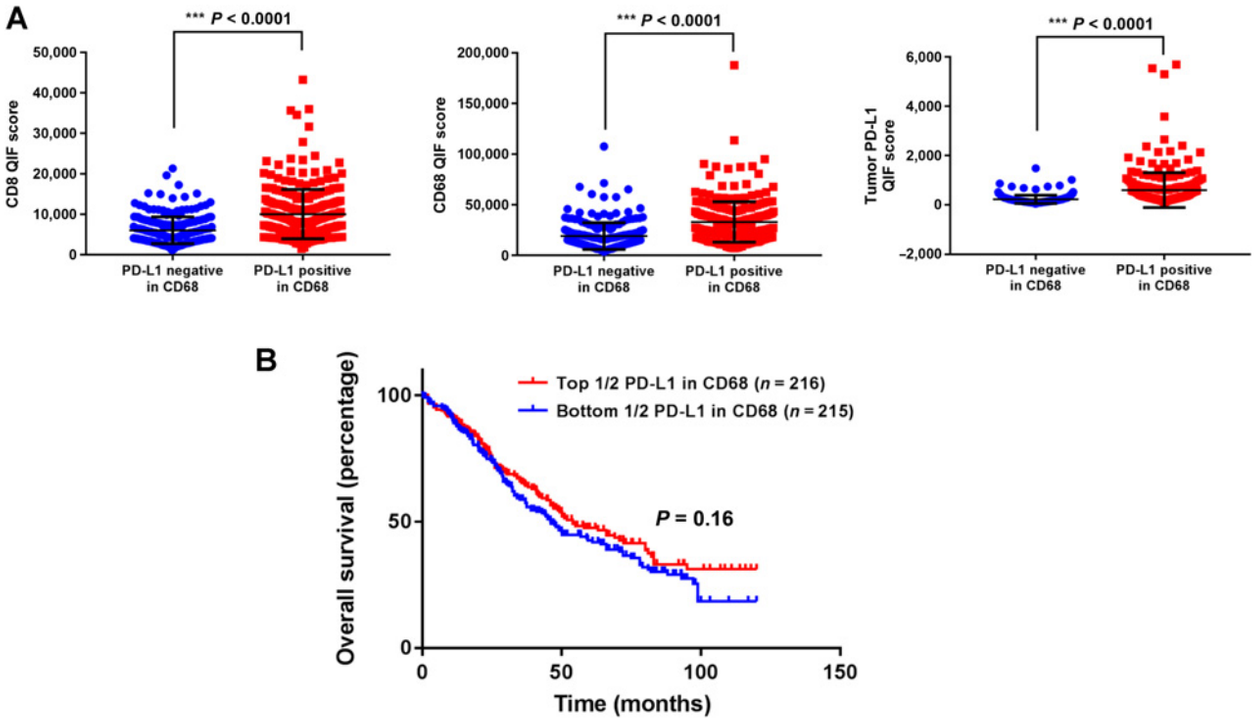

Figure 3.

A, High PD-L1 expression in macrophages was correlated with high CD8 level, high CD68 level, and high PD-L1 expression by tumor cells in 457 cases of NSCLC. **B,** Error bars represent mean with 95% confidence interval. PD-L1 expression in macrophages is not prognostic in this cohort.

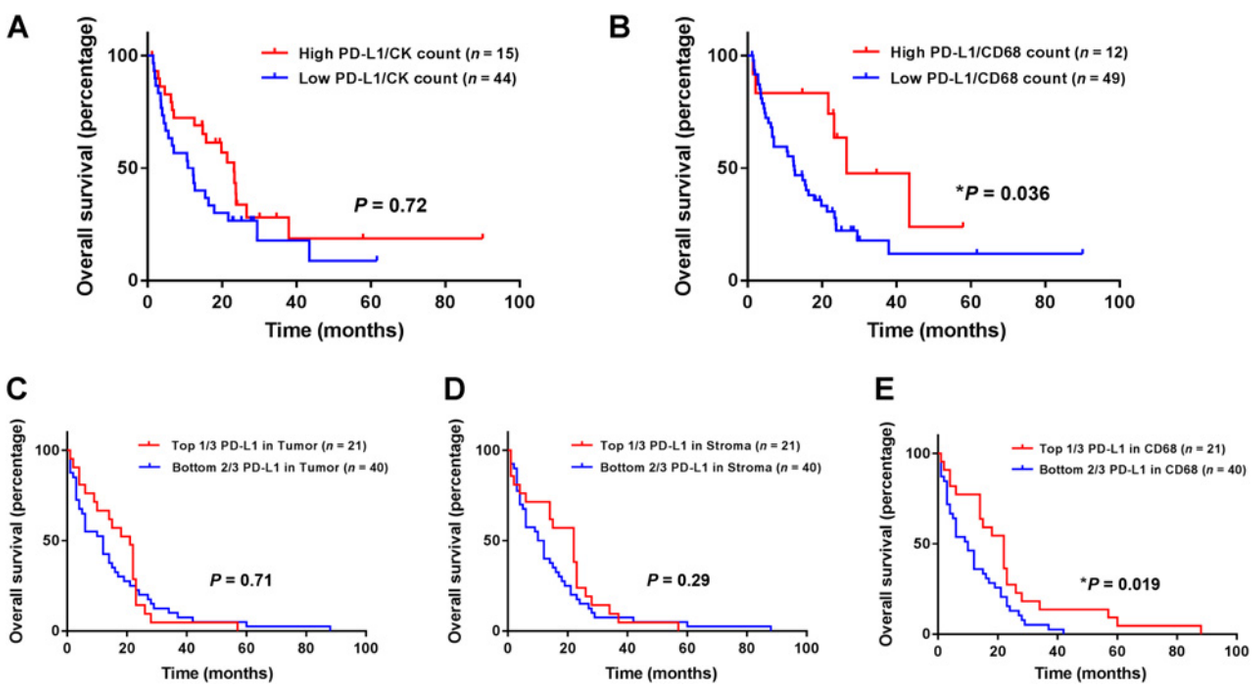

Figure 4.

PD-L1 level in macrophages predicts patients' OS to anti-PD-1 axis blockade therapy using two different QIF methods. **A,** Using InForm to count cells, double positive PD-L1 and CK cell (count $n = 15$) was not associated with OS. **B,** Double positive PD-L1/CD68 cells (count $n = 12$) were significantly associated with OS of patients with NSCLC treated with single-drug immunotherapy. Using AQUA assessment of PD-L1 in the tumor (**C**) or stromal (**D**) compartments was not associated with better outcome on monotherapy, while PD-L1 in the CD68 compartment was statistically significantly associated with better OS (**E**).

panel detect PD-L1, CD68, CD8, and CK. An AQUA-based analysis was done to measure PD-L1 expression in the stroma, tumor, and CD68-defined compartments. When assessed in tertiles, only PD-L1 in the CD68 compartment shows significance ($P = 0.019$; **Fig. 4C–E**).

Besides PD-L1 expression in $CD68^+$ cells, the level of CD8 was also found to be associated with response to immunotherapy (Supplementary Fig. S6). When assessed in quartiles, high level of CD8 is found to be significantly associated with better OS ($P = 0.0045$).

Discussion

Mechanistic studies have examined the function of PD-L1 expression in macrophages in mouse models and demonstrated that PD-L1 expression in host cells influenced PD-L1 blockade therapy (10–12), but few studies have examined the expression of PD-L1 in human tumors, beyond their general characterization as "immune cells". In this study, we evaluated the PD-L1 colocalization in three immune cell subtypes in 457 NSCLC patients' tissue and show that the majority of PD-L1 expression is in $CD68^+$ macrophages, as confirmed by two methods of QIF and confocal microscopy. Furthermore, expression of PD-L1 in macrophages was correlated with better OS in patients treated with immunotherapy.

PD-L1 has been found to be expressed not just by macrophages, cytotoxic T cells, and NK cells, but rather broadly expressed by hematopoietic and non-hematopoietic cells, including B cells, dendritic cells, regulatory T cells, etc (23–25). In addition, early stage tumor associated macrophages have been found to express both M1 and M2 markers thus the traditional M1/M2 associations with aggressiveness, or lack thereof, are not found (26, 27). While early-stage TAMs are associated with increased probability of recurrence and they have no effect on T cells (26, 28). It has been suggested that PD-L1 expressed by TAMs in early-stage lung cancer does not inhibit effector T-cell function (26).

With our current panels, we were able to demonstrate that the majority of PD-L1 expression by nonneoplastic cells were from $CD68^+$ cells that are likely to be classified as macrophages. Garris and colleagues have recently shown that the efficacy of anti-PD-1 immunotherapy requires intratumoral dendritic cells (29). One possible explanation is that dendritic cells can express PD-L1 and bind to PD-1 thus resulting in downstream immune inhibition. We have been unable to assess the percentage of PD-L1 in dendritic cells due to the absence of a definitive, single antibody dendritic cell marker. These findings suggest further translational studies on the role PD-L1 in other types of immune cells and its predictive value to immunotherapy with treated cohort.

There are several limitations to this study. Perhaps the greatest limitation is that this work is entirely performed on TMAs that may over or underrepresent the biomarker expression in whole-tissue section (WTS) because of tumor and microenvironmental heterogeneity. However, study has shown good concordance between TMAs and corresponding whole-tissue section and between two TMA cores from two paraffin blocks of the same tumor in breast cases (30). Moreover, previous work in our laboratory assessed the PD-L1 QIF score in TMA cases and compared it with the corresponding WTS cases. We found a comparable PD-L1 detection between TMA and WTS in NSCLC cohorts (31). The advantage of large numbers of cases accessible by TMA is favored here. A second limitation is the relatively small size of the immunotherapy-treated cohort and the heterogeneity of treatment of this cohort. Access to tissue from treated patients is limited and similarly long-term follow-up is just now becoming available for treatment of patients with these medications after their FDA approval and acceptance as standard of care. As such this work should be considered as preliminary and should be validated by larger prospective studies.

Another concern is that the tissue used in this study was archival tissue, not collected specifically for companion diagnostic testing. The issue of antigen aging has recently been addressed by Herbst and colleagues and suggests that this concern does appear to affect the predictive value of the PD-L1 test (32). Finally, CD68 may not stain all tumor-associated macrophages and CD56 may also capture NKT cells. As such, this data must be considered hypothesis generating, or discovery data and the observation that PD-L1 expression in macrophages as the key predictive factor requires validation in external cohorts, or potentially future clinical trials.

In summary, we find PD-L1 expression is particularly frequent in macrophages as compared with other immune cell types in patients with NSCLC. Elevated level of PD-L1 in macrophages could be evaluated in future studies as potentially contributory to the therapeutic efficacy of anti-PD-1 blockade therapy.

Disclosure of Potential Conflicts of Interest

J. Zugazagoitia reports receiving speakers bureau honoraria from and is an unpaid consultant/advisory board member for Guardant Health. B.S. Henick is an employee/paid consultant for Boehringer Ingelheim and holds ownership interest (including patents) in Abbvie. S.N. Gettinger is an employee/paid consultant for Bristol-Myers Squibb. R.S. Herbst is an employee/paid consultant for Abbvie Pharmaceuticals, ARMO Biosciences, AstraZeneca, Biodesix, Bolt Biotherapeutics, Bristol-Myers Squibb, Eli Lilly and Company, EMD Serrano, Genentech/Roche, Genmab, Halozyme, Heat Biologics, IMAB Biopharma, Immunocore, Loxo Oncology, Merck and Company, Midas Health Analytics, Nektar, NextCure, Novartis, Pfizer, Sanofi, Seattle Genetics, Shire PLC, Spectrum Pharmaceuticals, Symphogen, Takeda, Tesaro, Tocagen, and Junshi Pharmaceuticals; reports receiving commercial research grants from AstraZeneca, Eli Lilly and Company, and Merck and Company; and is an unpaid consultant/advisory board member for Neon Therapeutics, Infinity Pharmaceuticals, and NextCure. K.A. Schalper is an employee/paid consultant for Clinica Alemana Santiago, Celgene, Moderna Therapeutics, Shattuck Labs, Pierre Fabre, AstraZeneca, Dynamo Therapeutics, EMD Serono, and Takeda; reports receiving commercial research grants from Navigate BP, Tesaro, Takeda, Surface Oncology, Pierre Fabre, Merck, Bristol-Myers Squibb, AstraZeneca, and Eli Lilly; and reports receiving speakers bureau honoraria from Merck, Bristol-Myers Squibb, Fluidgm, and Takeda. D.L. Rimm is an employee/paid consultant for AstraZeneca, Bristol-Myers Squibb, Merck, and Roche, and reports receiving commercial research grants from AstraZeneca, and Ultivue. No potential conflicts of interest were disclosed by the other authors.

Disclaimer

The funding sources had no role in study design; collection, analysis, and interpretation of data; preparation of the article; or the decision to submit for publication.

Authors' Contributions

Conception and design: Y. Liu, B.S. Henick, S.N. Gettinger, R.S. Herbst, D.L. Rimm
Development of methodology: Y. Liu, J. Zugazagoitia, R.S. Herbst, K.A. Schalper, D.L. Rimm
Acquisition of data (provided animals, acquired and managed patients, provided facilities, etc.): Y. Liu, J. Zugazagoitia, S.N. Gettinger, R.S. Herbst
Analysis and interpretation of data (e.g., statistical analysis, biostatistics, computational analysis): Y. Liu, J. Zugazagoitia, F.S. Ahmed, B.S. Henick, S.N. Gettinger, R.S. Herbst, K.A. Schalper, D.L. Rimm
Writing, review, and/or revision of the manuscript: Y. Liu, J. Zugazagoitia, F.S. Ahmed, B.S. Henick, S.N. Gettinger, R.S. Herbst, K.A. Schalper, D.L. Rimm
Administrative, technical, or material support (i.e., reporting or organizing data, constructing databases): Y. Liu, D.L. Rimm
Study supervision: D.L. Rimm
Other (experimentation): F.S. Ahmed

Acknowledgments

This work was primarily supported by funds from Yale SPORE in Lung Cancer (to R.S. Herbst, K.A. Schalper, S.N. Gettinger, and D.L. Rimm, P50-CA196530) and also funds from the Yale Cancer Center (P30CA016359) and funds from Navigate BioPharma (Novartis subsidiary) to D.L. Rimm and K.A. Schalper.

The costs of publication of this article were defrayed in part by the payment of page charges. This article must therefore be hereby marked *advertisement* in accordance with 18 U.S.C. Section 1734 solely to indicate this fact.

Received March 27, 2019; revised July 18, 2019; accepted October 10, 2019; published first October 15, 2019.

References

1. Sharpe AH, Wherry EJ, Ahmed R, Freeman GJ. The function of programmed cell death 1 and its ligands in regulating autoimmunity and infection. Nat Immunol 2007;8:239–45.
2. Pardoll DM. The blockade of immune checkpoints in cancer immunotherapy. Nat Rev Cancer 2012;12:252–64.
3. Ribas A. Adaptive immune resistance: how cancer protects from immune attack. Cancer Discov 2015;5:915–9.
4. Dong H, Strome SE, Salomao DR, Tamura H, Hirano F, Flies DB, et al. Tumor-associated B7-H1 promotes T-cell apoptosis: a potential mechanism of immune evasion. Nat Med 2002;8:793–800.
5. Freeman GJ, Long AJ, Iwai Y, Bourque K, Chernova T, Nishimura H, et al. Engagement of the PD-1 immunoinhibitory receptor by a novel B7 family member leads to negative regulation of lymphocyte activation. J Exp Med 2000; 192:1027–34.
6. Zou W, Wolchok JD, Chen L. PD-L1 (B7-H1) and PD-1 pathway blockade for cancer therapy: mechanisms, response biomarkers, and combinations. Sci Transl Med 2016;8:328rv4.
7. Gettinger SN, Horn L, Gandhi L, Spigel DR, Antonia SJ, Rizvi NA, et al. Overall survival and long-term safety of nivolumab (anti-programmed death 1 antibody, BMS-936558, ONO-4538) in patients with previously treated advanced non-small-cell lung cancer. J Clin Oncol 2015;33:2004–12.
8. Herbst RS, Soria JC, Kowanetz M, Fine GD, Hamid O, Gordon MS, et al. Predictive correlates of response to the anti-PD-L1 antibody MPDL3280A in cancer patients. Nature 2014;515:563–7.
9. Udall M, Rizzo M, Kenny J, Doherty J, Dahm S, Robbins P, et al. PD-L1 diagnostic tests: a systematic literature review of scoring algorithms and test-validation metrics. Diagn Pathol 2018;13:12.
10. Tang H, Liang Y, Anders RA, Taube JM, Qiu X, Mulgaonkar A, et al. PD-L1 on host cells is essential for PD-L1 blockade-mediated tumor regression. J Clin Invest 2018;128:580–8.
11. Lin H, Wei S, Hurt EM, Green MD, Zhao L, Vatan L, et al. Host expression of PD-L1 determines efficacy of PD-L1 pathway blockade-mediated tumor regression. J Clin Invest 2018;128:805–15.
12. Lau J, Cheung J, Navarro A, Lianoglou S, Haley B, Totpal K, et al. Tumour and host cell PD-L1 is required to mediate suppression of anti-tumour immunity in mice. Nat Commun 2017;8:14572.
13. Schalper KA, Brown J, Carvajal-Hausdorf D, McLaughlin J, Velcheti V, Syrigos KN, et al. Objective measurement and clinical significance of TILs in non-small cell lung cancer. J Natl Cancer Inst 2015;107. doi: 10.1093/jnci/dju435.
14. Altan M, Pelekanou V, Schalper KA, Toki M, Gaule P, Syrigos K, et al. B7-H3 expression in NSCLC and its association with B7-H4, PD-L1 and tumor-infiltrating lymphocytes. Clin Cancer Res 2017;23:5202–9.
15. McCabe A, Dolled-Filhart M, Camp RL, Rimm DL. Automated quantitative analysis (AQUA) of in situ protein expression, antibody concentration, and prognosis. J Natl Cancer Inst 2005;97:1808–15.
16. Camp RL, Chung GG, Rimm DL. Automated subcellular localization and quantification of protein expression in tissue microarrays. Nat Med 2002;8: 1323–7.
17. Brown JR, Wimberly H, Lannin DR, Nixon C, Rimm DL, Bossuyt V, et al. Multiplexed quantitative analysis of CD3, CD8, and CD20 predicts response to neoadjuvant chemotherapy in breast cancer. Clin Cancer Res 2014;20:5995–6005.
18. Pelekanou V, Villarroel-Espindola F, Schalper KA, Pusztai L, Rimm DL. CD68, CD163, and matrix metalloproteinase 9 (MMP-9) co-localization in breast tumor microenvironment predicts survival differently in ER-positive and -negative cancers. Breast Cancer Res 2018;20:154.
19. Gaule P, Smithy JW, Toki M, Rehman J, Patell-Socha F, Cougot D, et al. A quantitative comparison of antibodies to programmed cell death 1 ligand 1. JAMA Oncol 2017;3:256–9.
20. Tsao MS, Kerr KM, Kockx M, Beasley MB, Borczuk AC, Botling J, et al. PD-L1 immunohistochemistry comparability study in real-life clinical samples: results of blueprint phase 2 project. J Thorac Oncol 2018;13:1302–11.
21. Martinez-Morilla S, McGuire J, Gaule P, Moore L, Acs B, Cougot D, et al. Quantitative assessment of PD-L1 as an analyte in immunohistochemistry diagnostic assays using a standardized cell line tissue microarray. Lab Invest 2020;100:4–15.
22. Kim HJ, Fay MP, Feuer EJ, Midthune DN. Permutation tests for joinpoint regression with applications to cancer rates. Stat Med 2000;19:335–51.
23. Dorfman DM, Brown JA, Shahsafaei A, Freeman GJ. Programmed death-1 (PD-1) is a marker of germinal center-associated T cells and angioimmunoblastic T-cell lymphoma. Am J Surg Pathol 2006;30:802–10.
24. Curiel TJ, Wei S, Dong H, Alvarez X, Cheng P, Mottram P, et al. Blockade of B7-H1 improves myeloid dendritic cell-mediated antitumor immunity. Nat Med 2003;9:562–7.
25. Francisco LM, Sage PT, Sharpe AH. The PD-1 pathway in tolerance and autoimmunity. Immunol Rev 2010;236:219–42.
26. Singhal S, Stadanlick J, Annunziata MJ, Rao AS, Bhojnagarwala PS, O'Brien S, et al. Human tumor-associated monocytes/macrophages and their regulation of T cell responses in early-stage lung cancer. Sci Transl Med 2019;11. doi: 10.1126/scitranslmed.aat1500.
27. Lavin Y, Kobayashi S, Leader A, Amir ED, Elefant N, Bigenwald C, et al. Innate immune landscape in early lung adenocarcinoma by paired single-cell analyses. Cell 2017;169:750–65.
28. Mony JT, Schuchert MJ. Prognostic implications of heterogeneity in intra-tumoral immune composition for recurrence in early stage lung cancer. Front Immunol 2018;9:2298.
29. Garris CS, Arlauckas SP, Kohler RH, Trefny MP, Garren S, Piot C, et al. Successful anti-PD-1 cancer immunotherapy requires T cell-dendritic cell crosstalk involving the cytokines IFN-gamma and IL-12. Immunity 2018;49: 1148–61.
30. Kyndi M, Sorensen FB, Knudsen H, Overgaard M, Nielsen HM, Andersen J, et al. Tissue microarrays compared with whole sections and biochemical analyses. A subgroup analysis of DBCG 82 b&c. Acta Oncol 2008;47:591–9.
31. McLaughlin J, Han G, Schalper KA, Carvajal-Hausdorf D, Pelekanou V, Rehman J, et al. Quantitative assessment of the heterogeneity of PD-L1 expression in non-small-cell lung cancer. JAMA Oncol 2016;2:46–54.
32. Herbst RS, Baas P, Perez-Gracia JL, Felip E, Kim DW, Han JY, et al. Use of archival versus newly collected tumor samples for assessing PD-L1 expression and overall survival: an updated analysis of KEYNOTE-010 trial. Ann Oncol 2019;30:281–9.